



A prudent approach for the removal of copper (II) and cadmium (II) ions from aqueous solutions using indigenous *Macrae aequisulcata* shells

SYED MUHAMMAD REHAN ULLAH^{1,2*}, ERUM ZAHIR²
and MUHAMMAD ASIF ASGHAR³

¹Department of Chemical Oceanography & Marine Environment, National Institute of Oceanography, St-47, Block-1 Clifton, Karachi-75600, Sindh-74200, Pakistan, ²Department of Chemistry, University of Karachi, Karachi-75270, Sindh-74200, Pakistan and ³Food and Feed Safety Laboratory, Food and Marine Resources Research Centre, PCSIR Laboratories Complex, Shahrah-e-Salimuzzaman Siddiqui, Off University Road, Karachi-75280, Sindh-74200, Pakistan

(Received 28 December 2020, revised 22 March, accepted 4 April 2021)

Abstract: In this study, the raw seashells of *Macrae aequisulcata*, of the class Bivalvia and the phylum Mollusca were employed as an adsorbent to remove copper (II) and cadmium (II) metal ions from aqueous solution. The characterization of shells was performed using FTIR, EDX and SEM, BET isotherm and point of zero charge (pH_{pzc}). Batch experiments were performed to assess various factors on the biosorption efficiency. Maximum adsorption of both metals ions conveniently found at 0.4 g L⁻¹ adsorbent dose, pH 5 and at 303 K. Maximum biosorption capacities for Cu²⁺ and Cd²⁺ were 59.57 and 38.12 mg g⁻¹, respectively. The Langmuir isotherm model was found to be the best fit for the acquired equilibrium data. Thermodynamic and kinetic parameters showed that the process was feasible, exothermic and followed pseudo-first order.

Keywords: adsorbent; heavy metals; pollutants; remediation; wastewater.

INTRODUCTION

The environmental condition for humans and other living beings worldwide has become more inhospitable than it has ever been before.¹ The industrial activities have posed series threats to the environment. Technological advancements and rapid consumption have led to various genres of pollution.² The discharge of industrial effluent bearing heavy metals causes great adversities due to their presence and ability to accumulate and toxic effects on living things.³ As far as environmental threat is concerned, toxic heavy and radionuclides metals are of main concern and ought to be nullified. Toxic metal ions can cause minor

* Corresponding author. E-mail: rehan-syed@outlook.com
<https://doi.org/10.2298/JSC201228028U>

discomforts as well as life threatening illnesses by irreversible damage of vital body systems. Eco-toxicologically, most toxic metals are cadmium, chromium, lead and mercury. Heavy metals can bioaccumulate as well as biomagnify in the food chain. So, their toxicities are more noticeable in the animals that are in high trophic levels.⁴ Currently, various techniques are used to remediate waste water from these toxic metals. Adsorption processes have been proven to be a better technique as compared with other techniques, namely electrochemical, oxidation, membrane filtration, ozonization and complexation. It has also greater importance due to operational easiness, relatively low cost, and simplicity of design in the decoloration process.⁵ Mollusca shells are mostly composed of aragonite and calcite type calcium carbonate, that's around 95–99 % of entire shell quantity, and also contains a small amount of organic matter.⁶ The seashells as an agent to remediate wastewater from heavy metals have also been employed, rather than geological calcium carbonate.⁷ Biosorption augmentation through pre-treatment processes, such as with organic chemicals,⁵ thermal processing⁸ and acid treatment⁹ have also been successfully opted. *Mactra aequisulcata*, species of mussels, found in marine habitat, has aragonite as its major constituent¹⁰ and biogenic aragonite is considered to be a suitable biosorbent for heavy metal adsorption⁹. Moreover, the aforementioned species has not been reported for the remediation of heavy metals in the aqueous medium as well from industrial effluents, and not any mussels' species locally, for that matter. Considering the aforementioned approaches, the study was designed to assess the biosorption capability of pulverized *Mactra aequisulcata* shells to remove Cu²⁺ and Cd²⁺ from the aqueous phase. Optimal adsorption process was assessed by varying in adsorbent dose, interaction time, metals initial concentration, pH and temperature. The biosorption mechanism was conducted in terms of isotherm models, kinetics and thermodynamics studies.

EXPERIMENTAL

Materials

The chemicals employed in this research were of analytical grade. Millipore Q5 Direct water purification system was used to prepare deionized water with conductivity of 0.06 $\mu\text{S cm}^{-1}$. *Mactra aequisulcata* (Class Bivalvia, Phylum Mollusca, 100 units) were sampled from the Clifton Beach, Karachi city of Pakistan and stored in a pre-washed plastic ziplocks. The seashells were washed with tap water, then immersed into 0.5 % of HCl solution for 30 min, for the removal of impurities adhered on the surface of shells. The shells were washed with DI-H₂O repeatedly, drying in an oven at 80 °C and pulverized to powder form using 500 g electric grain grinder mill. The pulverized adsorbent was kept in polyethylene airtight vessels in ambient condition. The preparation of working stock solutions of Cu²⁺ and Cd²⁺ was done with CuSO₄ 5H₂O and CdCl₂ (>99 %, Merck, Germany), respectively. The solution pH were altered to the desired level with 0.1 M HCl and NaOH.

Biosorption of metal ions

For metals biosorption, a known quantity of pulverized seashell was used with 50 mL of Cu²⁺ and Cd²⁺ solutions in an Erlenmeyer flask, separately. The outcome of the adsorbent dose (0.2, 0.4, 0.6, 0.8 and 1.0 g L⁻¹), initial metals ions concentration (5, 10, 25, 50 and 100 mg L⁻¹), initial pH of metal solutions (2, 3, 4, 5 and 6), interaction time (10, 20, 30, 40 and 60 min) and temperature (303, 308, 313, 318 and 323 K) were studied. After each experiment, the solutions were filtered using Whatman filter paper no. 42. Controlled sample without the addition of biosorbent, was also quantified to assess the interference of filter papers, and no interference was observed. The filtrate was used to determine the heavy metal ions concentrations using atomic absorption spectrometer. The percentage of metal adsorption and maximum biosorption capacity, q in mg g⁻¹, were measured using the following equations:

$$ADS = 100 \frac{C_0 - C_e}{C_0} \quad (1)$$

$$q = \frac{V(C_0 - C_e)}{m} \quad (2)$$

where, C_0 and C_e in mg L⁻¹, correspond to the initial and equilibrium concentrations of the metals ions, respectively, m is the mass of the biosorbent in mg and V is volume of the solution in L.

Instrumentation

The Cu²⁺ and Cd²⁺ in the samples were quantified with atomic absorption spectrometry (PinAACle 900T, Perkin Elmer). Eutech Cyber Scan PCD 650 was used for the pH measurements. An electric grain grinder mill was used to grind the seashells. The availability of functional groups in the ground seashell samples was determined with Fourier transform infrared spectrophotometry (FTIR, Perkin Elmer, Singapore). The surface area was evaluated through Autosorb-1 Quantachrome, Asiawin. The morphology of the surface and diameter of ground seashell were examined using SEM (JSM 6380A, JEOL Ltd, Japan). The deduction of elemental composition was carried with EDX spectroscopy (EX-54175 JMU, JEOL Ltd, Tokyo, Japan).

Determination of pH_{pzc}

The point of zero charge (pH_{pzc}) of the pulverized *M. aequisulcata* shells was determined by taking six separate Erlenmeyer flasks containing 50 ml 0.1 M NaCl having pH 2, 4, 6, 8, 10 and 12. The pH of the solutions were adjusted by adding 1 M HCl or 1 M NaOH. To each flask, 0.1 g pulverized shell powder was added and then the capped flasks were shaken at 150 rpm for 4 h. The suspensions were filtered with the Whatman filter paper no. 42. The difference between initial pH (pH_i) and the final pH (pH_f) was plotted with pH_i. The intersection of the plot and pH_i (x-axis) was deemed as the pH_{pzc}.

Biosorption isotherm models

For isotherm studies, an adsorbent dose of 0.4 g L⁻¹ of pulverized seashell was used with 50 mL of Cu²⁺ and Cd²⁺ solutions in Erlenmeyer flasks, separately; with initial adsorbate concentrations of 5, 10, 25, 50 and 100 mg L⁻¹, initial pH of 5, at 303 K, and interactions time of 20 and 30 min for Cu²⁺ and Cd²⁺, respectively. The isotherm explains how metal ions concentrations and sorbed metal amount interact on the solid surface at their equilibrium phases. In this work, the biosorption specifics were studied by Langmuir, Freundlich and Temkin isotherm models. Langmuir isotherm details about the monolayer adsorption and states the abs-

ence of lateral interaction between the adsorbate molecules. The nonlinear Langmuir isotherm model is expressed as follows:¹¹

$$q_e = \frac{q_m b C_e}{1 + b C_e} \quad (3)$$

where, C_e in mg L⁻¹ signifies the equilibrium concentration of the metal ions, q_e in mg g⁻¹, corresponds to the equilibrium adsorption capacity, q_m in mg g⁻¹ and b in L mg⁻¹, are the Langmuir constants relating to adsorption capacity and energy, respectively.

The favourability of adsorption process can be predicted by the assessment of Langmuir essential characteristic denoted as the separation factor, R_L and its equation is illustrated as:¹²

$$R_L = \frac{1}{1+bC_0} \quad (4)$$

The Freundlich model, nonlinear form is applicable to multilayer adsorption, relating to energetic surface heterogeneity and can be assessed from the following equation:¹³

$$q_e = K_f C_e^{1/n} \quad (5)$$

where K_f / mg g⁻¹ (L mg⁻¹)^{1/n} and $1/n$ correspond to the Freundlich constants of adsorption capacity and heterogeneity factor, respectively.

The following equation illustrates the Temkin isotherm nonlinear model (Eq. 6):

$$q_e = B \ln (A_T C_e) \quad (6)$$

where, B in J mol⁻¹, is the constant of heat of sorption at equilibrium and A_T in L g⁻¹, being the binding constant. The Temkin isotherm illustrates that the heat of adsorption of every molecule in the layer decreases directly with increased surface coverage.¹⁴ Dubinin–Radushkevich model considers the adsorption of subcritical vapours on microporous adsorbent followed by the mechanism of pore filling, and is applicable to detail the mechanism of adsorption on heterogeneous surfaces with the Gaussian energy distribution.

The nonlinear Dubinin–Radushkevich model is represented as¹⁵:

$$q_e = q_s e^{-K_{DR} \varepsilon^2} \quad (7)$$

$$\varepsilon = RT \ln \left(1 + \frac{1}{C_e} \right) \quad (8)$$

where, q_s in mg g⁻¹ is the Dubinin–Radushkevich isotherm model constant relating to maximum adsorption capacity; K_{DR} , mol² kJ⁻², is Dubinin–Radushkevich isotherm constant; ε is the Polanyi potential, R / J mol⁻¹ K⁻¹; and T / K are the gas constant and absolute temperature, respectively.

Biosorption kinetics

For kinetics studies, an adsorbent dose of 0.4 g L⁻¹ of pulverized seashell was used with 50 mL of Cu²⁺ and Cd²⁺ solutions in Erlenmeyer flasks, separately; with initial metal ions concentration of 100 mg L⁻¹, initial pH of 5, at 303 K, and over the period of 10, 20, 30, 40 and 60 min. The two most important nonlinear kinetic models: *i*) pseudo-first order (Eq. (7)) and *ii*) pseudo-second order (Eq. (8)) are described by the equations as follows:

$$q_t = q_e (1 - e^{-k_1 t}) \quad (9)$$

$$q_t = \frac{q_e^2 k_2 t}{q_e k_2 t + 1} \quad (10)$$

k_1 / min^{-1} and $k_2 / \text{g mg}^{-1} \text{ min}^{-1}$ are the rate constants of pseudo-first order and pseudo-second order, respectively; and $q_t / \text{mg g}^{-1}$ is the amount of metal ion adsorbed at any given time t .

Biosorption thermodynamics

The nature of biosorption system was studied with thermodynamics analysis through van't Hoff equation. The following equations were applied for the deduction in the change in Gibbs energy, $\Delta G / \text{kJ mol}^{-1}$, entropy, $\Delta S / \text{kJ mol}^{-1} \text{ K}^{-1}$ and enthalpy, $\Delta H / \text{kJ mol}^{-1}$:

$$\ln K_c = \left(\frac{\Delta S}{R} \right) - \left(\frac{\Delta H}{RT} \right) \quad (11)$$

$$\Delta G = RT \ln K_c \quad (12)$$

where, K_c represents the constant of thermodynamic equilibrium and R corresponds to the Universal gas constant and T / K is the absolute temperature.

RESULTS AND DISCUSSION

Analysis and characterization of seashell

The Cu^{2+} and Cd^{2+} concentrations in the seashells were found to be well below the lower limit of quantitation (0.1 and 0.01 mg L^{-1} for Cu^{2+} and Cd^{2+} , respectively) of the utilized method. The results signified that the biosorbents would not interfere during the biosorption process as they do not have heavy metals in them. The functional groups in seashell powder sample were deduced by FTIR spectroscopy as illustrated in (Fig. 1). The various peaks appeared in the spectrum at 1789, 1455, 1076, 854, and 726 cm^{-1} and considered the specific features of CO_3^{2-} in CaCO_3 . The aragonite content of CaCO_3 in the sample was confirmed with the observance of a signal at 1076 cm^{-1} .¹⁶

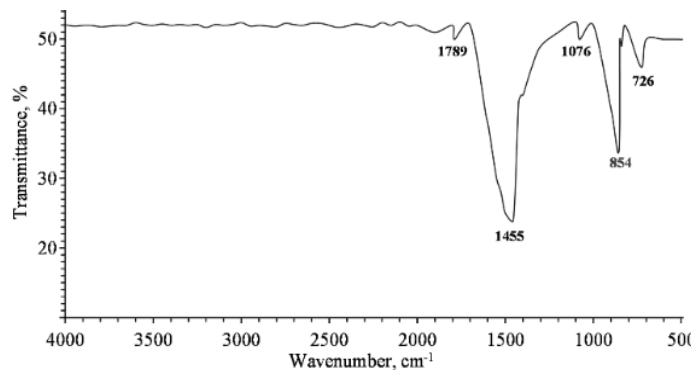


Fig. 1. FTIR spectrum of *M. aequisulcata* seashell powder.

The BET isotherm demonstrated that the biosorbent bears a small BET specific surface area ($1.77 \text{ m}^2 \text{ g}^{-1}$) and median pore width of 134.1 nm. Similarly, researchers^{17,18} have also deducted that CaCO_3 -rich biosorbents possess

low S_{BET} values. Hence, here, the surface area cannot be considered as a determining factor for the biosorption of cadmium and copper⁹. The morphology of the surfaces of pulverized, Cu^{2+} and Cd^{2+} laden seashell powders, were observed using SEM analysis and presented in Fig. 2a–c. It was evident that the surface of seashell powder (Fig. 2a) was heterogeneously distributed with slight grains and spaces. The copper ions SEM image (Fig. 2b) shows some sort of similarity with the adsorbent SEM image with tightly packed particles, and the presence of secondary solids on the adsorbent surface, signifying the occurrence of surface precipitation. The similarity with the SEM image of the adsorbent could possibly be due to precipitation of Cu^{2+} with bicarbonates in the aqueous medium since the $CaCO_3$ dominant adsorbent tend to leach its constituents ions in the solvent medium, of which carbonates transform into bicarbonates.¹⁹ The SEM image of post-biosorption of Cd^{2+} (Fig. 2c) can be categorized as powder layered, showing precipitation on the surface. Cadmium adsorption on calcium carbonate compounds usually follows surface precipitation since ionic radii of the divalent calcium and cadmium are similar, as shown in the SEM image.¹⁸

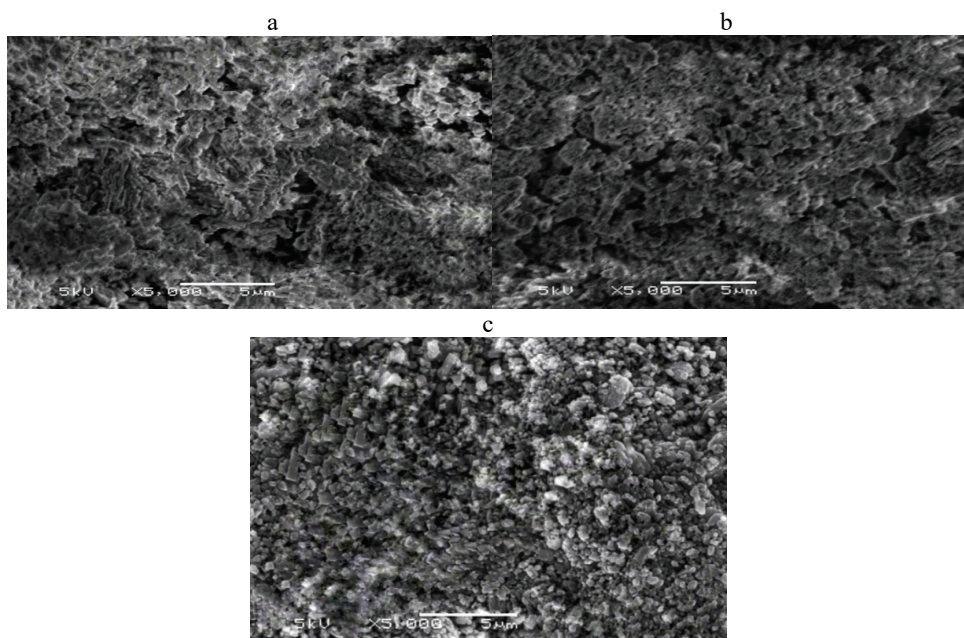


Fig. 2. SEM images of a – seashell powder, b – Cu^{2+} and c – Cd^{2+} laden seashell powder.

The pre and post adsorption elemental profiles of seashell powder are shown in Fig. 3a–c. The seashell powder EDX spectra (Fig. 3a) showed carbon, oxygen and calcium were the major constituents. The calcium-loaded adsorbent spectra (Fig. 3b) showed the addition of copper in the elemental profile signifying the

adsorption on the adsorbent, and the slight decrease in weight and atomic percentage of calcium indicate the surface precipitation of Cu^{2+} . The Cd^{2+} laden adsorbent EDX spectra (Fig. 3c) illustrated a small change in the elemental profiles of calcium and other elements, with only the addition of cadmium signal, indicating the aggregate formation, *i.e.*, $(\text{Cd}, \text{Ca})\text{CO}_3$.⁹

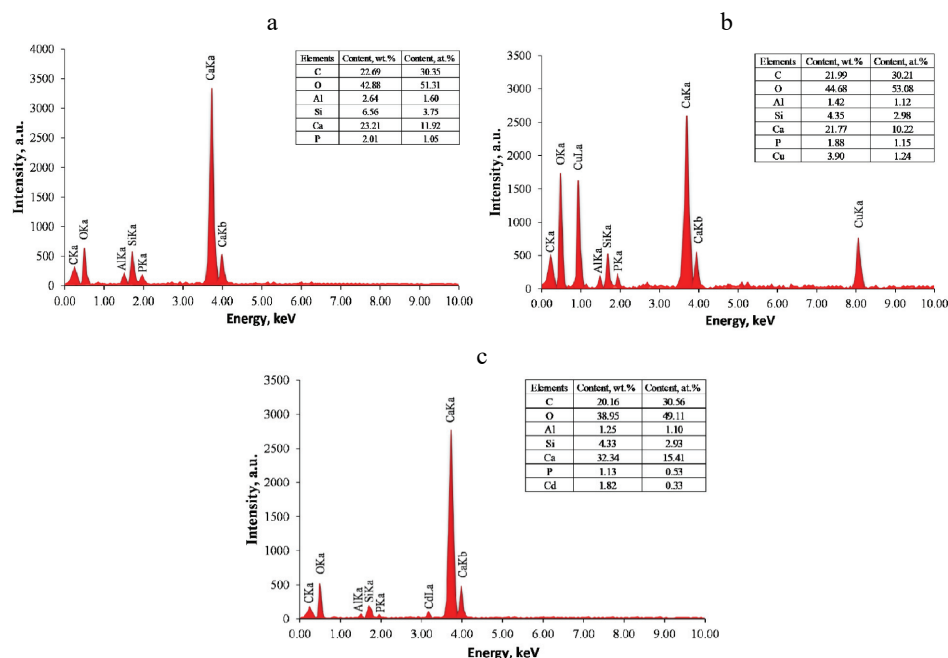


Fig. 3. EDX spectra of: a – seashell powder, b – Cu^{2+} and c – Cd^{2+} laden seashell powder.

The pH_{pzc} value of the adsorbent was found to be 9.25, signifying that the adsorbent surface was mostly positive. This result suggests that positively charged Cu^{2+} and Cd^{2+} couldn't easily adsorb onto the adsorbent through ion exchange and thus complexation or surface precipitation could be considered as the primary adsorption mechanism.²⁰

Adsorption study of metal ions using seashell

The Cu^{2+} and Cd^{2+} adsorption was performed with *M. aequisulcata* seashell. The biosorption efficacy was augmented by altering the metal ions concentrations, temperature of the process, pH and contact time.

Interaction time. Fig. 4 illustrates the plot of contact time, t in min, and percentage adsorption of Cu^{2+} and Cd^{2+} with *M. aequisulcata* shells. The plot shows that the metal uptake was rapid and the increase in biosorption capacity in the initial 20 min for Cu^{2+} and 30 min for Cd^{2+} , afterward no considerable variation was observed until 60 min. The fast process was due to involvement of the

biosorbent external surface in the metal ions adsorption. The next phase was slower as several of the external places were engaged.²

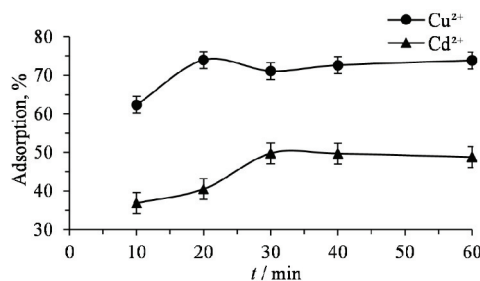


Fig. 4. Effect of contact time (t) on adsorption of Cu^{2+} and Cd^{2+} .

pH. A principal parameter for the assessment of the behavior of adsorbent–adsorbate is evaluation of the effect that changing pH confers onto adsorption. This was carried out from pH value 2 to 6. Fig. 5 is the plot between pH and percentage adsorption of Cu^{2+} and Cd^{2+} using pulverized seashells. The plots show that the metal ions uptake was very low at pH 2 but biosorption capacity increased till pH 5.0 and was constant after that, till pH 6.0 for both metals ions. The lower biosorption capacities were found in intense acidic pH ranges for both metal ions, reason being the protonation of the active places of the biosorbent in acidic media, therefore, decrease in metal ions biosorption was observed.²¹

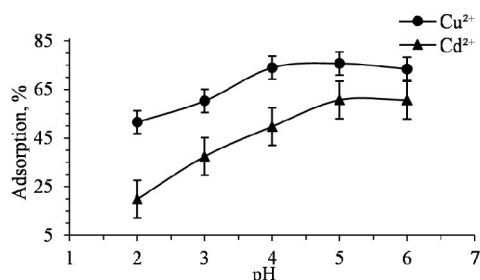


Fig. 5. Effect of initial pH on adsorption of Cu^{2+} and Cd^{2+} .

Adsorbent dose. Fig. 6 is the plot of adsorbent dose, g L^{-1} , and percentage adsorption of Cu^{2+} and Cd^{2+} using pulverized seashells. The plot shows that inc-

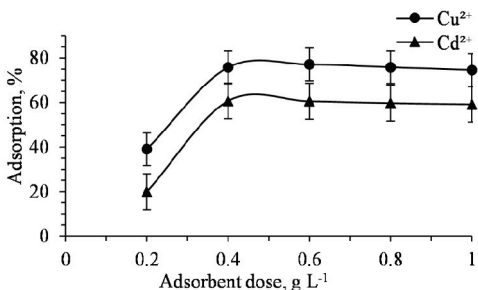


Fig. 6. Effect of adsorbent dose, on adsorption of Cu^{2+} and Cd^{2+} .

rease in adsorbent dose from 0.2–1.0 g L⁻¹ led to increase in biosorption efficiency, however, increase in adsorbent dose after 0.4 g L⁻¹ resulted in the decline in biosorption efficiency, this is due to the unsaturation of biosorption sites, particle interfaces, *i.e.*, accumulation and rarer energetic places at greater biosorbent doses.²

Biosorption isotherm models

The values obtained from calculating the equations (Eqs. (3–8)) are shown in Table I.

TABLE I. Langmuir, Freundlich, Temkin and Dubinin–Radushkevich isotherm models for the biosorption of Cu²⁺ and Cd²⁺ using *Mactra aequisulcata* seashells

Model	Parameter	Cu ²⁺	Cd ²⁺
	$q_{\text{exp}} / \text{mg g}^{-1}$	59.57	38.12
Langmuir isotherm	R^2	0.960	0.976
	$q_{\text{cal}} / \text{mg g}^{-1}$	59.98	40.14
	$b_L / \text{L mg}^{-1}$	0.227	0.37
Freundlich isotherm	R^2	0.864	0.801
	$K_f / \text{mg g}^{-1} (\text{L mg}^{-1})^{1/n}$	19.04	16.85
	n	3.69	4.86
Temkin isotherm	R^2	0.900	0.886
	$A_T / \text{L g}^{-1}$	2.25	7.76
	$B / \text{J mol}^{-1}$	231.22	286.56
Dubinin–Radushkevich isotherm	R^2	0.850	0.866
	$q_{\text{cal}} / \text{mg g}^{-1}$	46.00	36.10
	$K_{\text{DR}} / \text{mol}^2 \text{kJ}^{-2}$	1×10^{-6}	4×10^{-7}

Whereas, the biosorption isotherms are presented in Figs. 7 and 8 for Cu²⁺ and Cd²⁺. The equilibrium statistics were more suited to the Langmuir isotherm when compared to Freundlich, Temkin and Dubinin–Radushkevich isotherm

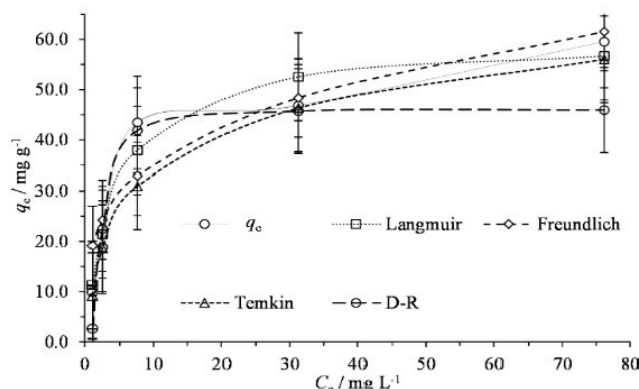


Fig. 7. Langmuir, Freundlich, Temkin and Dubinin–Radushkevich isotherm models for Cu²⁺ on seashell (*Mactra aequisulcata*) powder.

since the regression coefficient, R^2 values for Cu^{2+} and Cd^{2+} acquired by the Langmuir isotherm model were greater than other isotherm models, indicating monolayer adsorption and chemisorption.² The experimental q_{\max} values were observed as 59.98 and 40.14 mg g⁻¹ for Cu^{2+} and Cd^{2+} , respectively, according to the Langmuir isotherm model (Table I). These values were close with the biosorption capacities as calculated by Eq. (1) and found as 59.57 and 38.12 mg g⁻¹ for Cu^{2+} and Cd^{2+} , respectively. The R_L results were found to be 0.042 for Cu^{2+} and 0.027 for Cd^{2+} . The R_L values of over 0 and less than 1, for both metals ions, signify the favourability of biosorption process and Langmuir isotherm model.¹²

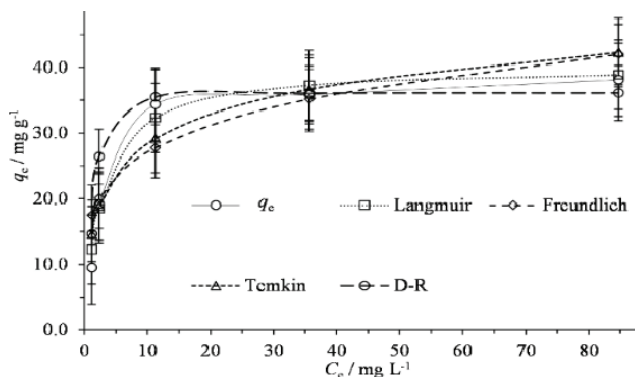


Fig. 8. Langmuir, Freundlich, Temkin and Dubinin–Radushkevich isotherm models for Cd^{2+} on seashell (*Mactra aequisulcata*) powder.

Biosorption kinetics

The biosorption rate is an essential factor to assess its reaction route. The adsorption data were assessed with the kinetic models using their respective equations (Eqs. (9) and (10)). The coefficients of correlation and calculated parameters are illustrated in Table II. The data (Table II) showed that pseudo-first order kinetic model described the adsorption processes for Cu^{2+} and Cd^{2+} better than the pseudo-second order model. The R^2 values of the pseudo-first order model were 0.961 and 0.970 and k_1 values were 0.160 and 0.08 min⁻¹ corresponding to Cu^{2+} and Cd^{2+} , respectively. The small values of k_1 for both metals ions refer to readily occupied adsorbent sites. The kinetic pseudo-first order model proposes fast adsorption in the initial stage and limiting step afterwards, referring to chemisorption. The metal ions uptake was rapid in the first 20 min for Cu^{2+} and 30 min for Cd^{2+} due to their high concentrations, the process slowed down gradually, since the precipitation involves nucleation and the growth of crystals on the adsorbent sites that were less available than before; a limiting step, due to rearrangement of atoms and bonds.²¹ The q_{\max} values were also in accordance with pseudo-first order kinetic model deduced q_e values, i.e.,

59.86 and 39.54 mg g⁻¹ for Cu²⁺ and Cd²⁺ and the R^2 values for the pseudo-order model being 0.820 and 0.911 for Cu²⁺ and Cd²⁺, respectively.

TABLE II. Kinetic parameters of Cu²⁺ and Cd²⁺ using *Mactra aequisulcata* seashells

Kinetic model	Parameter	Cu ²⁺	Cd ²⁺
	q_{exp} / mg g ⁻¹	59.57	38.12
Pseudo-first order	R^2	0.961	0.970
	k_1 / min ⁻¹	0.160	0.08
	q_{cal} / mg g ⁻¹	59.86	39.54
Pseudo-second order	R^2	0.820	0.911
	k_2 / g mg ⁻¹ min ⁻¹	0.005	0.002
	q_{cal} / mg g ⁻¹	64.46	47.74

Biosorption thermodynamics

The thermodynamic results of the biosorption are accessible in Table III. The negative values of ΔG values illustrating the spontaneity and feasibility of biosorption process.²² The attraction of the adsorbate towards the biosorbent is evaluated by K_c values and the maximum values for each ion were found at 303 K. Hence, all biosorption process were accomplished at this condition. The ΔG statistics raised with enhanced temperatures, demonstrating the prompt and more spontaneous biosorption process at lower temperatures. The ΔH values were -9.77 and -5.18 kJ mol⁻¹ for Cu²⁺ and Cd²⁺, respectively. The negative results showing that the biosorption was exothermic, at 303–323 K. The negative values of entropy showing a reduction in the disorderliness in ions biosorbed on the biosorbent in the solution. Accordingly, there were no further accessible ions contributing to the entropy in the solution.²

TABLE III. Thermodynamic parameters at different temperatures for the biosorption of Cu²⁺ and Cd²⁺ using *Mactra aequisulcata* seashells

Ion	T / K					ΔH / kJ mol ⁻¹	ΔS / kJ mol ⁻¹ K ⁻¹
	303	308	313	318	323		
ΔG / kJ mol ⁻¹							
Cu ²⁺	-3.39	-3.27	-3.17	-3.06	-2.97	-9.77	-0.02
Cd ²⁺	-1.74	-1.70	-1.64	-1.60	-1.50	-5.18	-0.01

Table IV illustrates the biosorption capacities of similar genre of biosorbents. The table also shows that the used biosorbent has the potential to be used as an efficient biosorbent due to its relatively better biosorption capacities.

CONCLUSION

This study intends to gauge intrinsic efficacy of the seashells for its diverse application. The easily found indigenous seashell, *Mactra Aequisulcata* of class Bivalvia was selected and successfully employed as a biosorbent to remove Cu²⁺

TABLE IV. An overview of biosorption capacities of different biosorbents of similar class.

Adsorbent	Material/polymorph	$q_e / \text{mg g}^{-1}$	Reference
Cu^{2+}			
<i>Anadara inaequivalvis</i> shells	Aragonite (CaCO_3)	330.2	²
<i>Mactra aequisulcata</i> shells	Aragonite (CaCO_3)	59.60	This study
<i>Chinonecetes opilio</i> (crab shell)	Protein, ash, lipid and chitin	55.90	²³
Bivalve mollusc shells	CaCO_3	38.93	²⁴
<i>Arca</i> shell	Biomass	17.64	²⁵
Cd^{2+}			
Apple snail shell	Aragonite (CaCO_3)	81.3	¹⁸
<i>Mactra aequisulcata</i> shells	Aragonite (CaCO_3)	38.1	This study
Mussel shells	Aragonite (CaCO_3)	28.6	⁹
<i>Corbicula fluminea</i> shell	Aragonite (CaCO_3)	4.03	²⁶
Crab shell	CaCO_3	3.43	²⁷
Oyster shell	CaCO_3	3.42	²⁸

and Cd^{2+} from aqueous phase. The maximum biosorption capacities were 59.6 and 38.1 mg g^{-1} at pH 5.0 for Cu^{2+} and Cd^{2+} , respectively. The acquired equilibrium data were best fitted with the Langmuir isotherm model. The biosorption showed spontaneity, followed pseudo-first order kinetics and was exothermic in nature. The kinetic study revealed quick uptake equilibrium at 20 and 30 min for Cu^{2+} and Cd^{2+} , respectively. Surface precipitation was deemed to be the primary adsorption mechanism. In conclusion, *M. aequisulcata* shells have the potential of a proficient biosorbent for the Cu^{2+} and Cd^{2+} removal from aqueous phase. Consequently, it can be used as economically and ecologically suitable biosorbent for heavy metals removal with reasonable biosorption capacity and abundance at industrial level.

SUPPLEMENTARY MATERIAL

Additional data are available electronically at the pages of journal website: <https://www.shd-pub.org.rs/index.php/JSCS/index>, or from the corresponding author on request.

И З В О Д

ПОУЗДАН ПРИСТУП УКЛАЊАЊУ ЈОНА БАКРА (II) И КАДМИЈУМА (II) ИЗ ВОДЕНИХ РАСТВОРА КОРИШЋЕЊЕМ АУТОХТОНИХ ШКОЉКИ *Mactra aequisulcata*

SYED MUHAMMAD REHAN ULLAH^{1,2}, ERUM ZAHIR² и MUHAMMAD ASIF ASGHAR³

¹Department of Chemical Oceanography & Marine Environment, National Institute of Oceanography, St-47, Block-1 Clifton, Karachi-75600, Sindh-74200, Pakistan, ²Department of Chemistry, University of Karachi, Karachi-75270, Sindh-74200, Pakistan и ³Food and Feed Safety Laboratory, Food and Marine Resources Research Centre, PCSIR Laboratories Complex, Shahrah-e-Salimuzzaman Siddiqui, Off University Road, Karachi-75280, Sindh-74200, Pakistan

Сирове школјке *Mactra aequisulcata*, класе Bivalvia и врсте Mollusca коришћене су као адсорбенс за уклањање металних јона бакра (II) и кадмијума (II) из воденог раствора. Карактеризација лјуштура извршена је помоћу FTIR, EDX и SEM методе, као и ВЕГ-изотерме и тачке нутлог наелектрисања (pH_{PZC}). Изведени су шаржни експерименти за процену различитих фактора на ефикасност биосорпције. Максимална адсорпција

оба метална јона нађена је при дози адсорбенса од $0,4 \text{ g L}^{-1}$, при pH 5 и 303 K. Максимални капацитет биосорпције за Cu^{2+} и Cd^{2+} био је 59,57 и $38,12 \text{ mg g}^{-1}$, редом. Утврђено је да се модел Ленгмирове изотерме показао као најприкладнији за добијене равнотежне податке. Термодинамички и кинетички параметри показали су да је процес изводљив, егзотерман и да прати псеудо-први ред.

(Примљено 28. децембра 2020, ревидирано 22. марта, прихваћено 4. априла 2021)

REFERENCES

1. K. Nahar, M. A. K. Chowdhury, M. A. H. Chowdhury, A. Rahman, K. M. Mohiuddin, *Environ. Sci. Pollut. Res.* **25** (2018) 7954 (<https://doi.org/10.1007/s11356-017-1166-9>)
2. S. K. Bozbaş, Y. Boz, *Process Saf. Environ. Prot.* **103** (2016) 144 (<https://doi.org/10.1016/j.psep.2016.07.007>)
3. D. Gola, A. Malik, Z. A. Shaikh, T. R. Sreekrishnan, *Environ. Process.* **3** (2016) 1063 (<https://doi.org/10.1007/s40710-016-0176-9>)
4. O. Abdi, M. Kazemi, *J. Mater. Environ. Sci.* **6** (2015) 1386 (https://www.jmaterenvironsci.com/Document/vol6/vol6_N5/164-JMES-1454-2015-Abdi.pdf)
5. B. Bano, E. Zahir, *Water Sci. Technol.* **73** (2015) 1301 (<https://doi.org/10.2166/wst.2015.590>)
6. R. R. Crichton, *Biological Inorganic Chemistry*, Elsevier, Milan, 2007, p. 330 (<https://doi.org/10.1016/B978-0-444-52740-0.X5024-8>)
7. Y. Du, F. Lian, L. Zhu, *Environ. Pollut.* **159** (2011) 1763 (<https://doi.org/10.1016/j.envpol.2011.04.017>)
8. E. Jeon, S. Ryu, S. Park, L. Wang, D. C. W. Tsang, *J. Clean. Prod.* **176** (2017) 54 (<https://doi.org/10.1016/j.jclepro.2017.12.153>)
9. H. T. Van, L. H. Nguyen, V. D. Nguyen, X. H. Nguyen, T. H. Nguyen, T. V. Nguyen, S. Vigneswaran, J. Rinklebe, H. N. Tran, *J. Environ. Manage.* **241** (2019) 535 (<http://hdl.handle.net/10453/128739>)
10. *Mactra aequisulcata* Sowerby Iii 1894 - Encyclopedia of Life (<https://eol.org/pages/46471883>), (28th January, 2021)
11. I. Langmuir, *J. Am. Chem. Soc.* **40** (1918) 136 (<https://doi.org/10.1021/ja02242a004>)
12. N. Ayawei, S. S. Angaye, D. Wankasi, E. D. Dikio, *Open J. Phys. Chem.* **5** (2015) 56 (<https://doi.org/10.4236/ojpc.2015.53007>)
13. H. Freundlich, *Z. Phys. Chem.* **57** (1907) 385 (<https://doi.org/10.1515/zpch-1907-5723>)
14. N. Ayawei, A. N. Ebelegi, D. Wankasi, *J. Chem.* **2017** (2017) (<https://doi.org/10.1155/2017/3039817>)
15. Z. Berizi, S. Y. Hashemi, M. Hadi, A. Azari, A. H. Mahvi1, *Water Sci. Technol.* **74** (2016) 1235 (<https://doi.org/10.2166/wst.2016.320>)
16. A. Shafiu Kamba, M. Ismail, T. A. Tengku Ibrahim, Z. A. B. Zakaria, *J. Nanomater.* **2013** (2013) (<https://doi.org/10.1155/2013/398357>)
17. D. Alidoust, M. Kawahigashi, S. Yoshizawa, H. Sumida, M. Watanabe, *J. Environ. Manage.* **150** (2015) 103 (<https://doi.org/10.1016/j.jenvman.2014.10.032>)
18. B. Zhao, J. E. Zhang, W. Yan, X. Kang, C. Cheng, Y. Ouyang, *Desalin. Water Treat.* **57** (2016) 23987 (<https://doi.org/10.1080/19443994.2016.1140078>)
19. A. Sdiri, T. Higashi, *Appl. Water Sci.* **3** (2013) 29 (<https://doi.org/10.1007/s13201-012-0054-1>)
20. H. N. Tran, S. You, H. Chao, *Waste. Manage. Res.* **34** (2016) 129 (<https://doi.org/10.1177/0734242x15615698>)

22. D. M. Veneu, C. L. Schneider, M. B. De Mello, O. Galvão, C. Cunha, L. Yokoyama, *Environ. Technol.* **39** (2018) 1670 (<https://doi.org/10.1080/09593330.2017.1336574>)
23. W. Wei, Q. Wang, A. Li, J. Yang, F. Ma, S. Pi, D. Wu, *Sci. Rep.* **6** (2016) 1 (<https://doi.org/10.1038/srep31575>)
24. A. Hossain, S. R. Bhattacharyya, G. Aditya, *Wat. Res.* **35** (2014) 3551 ([https://doi.org/10.1016/S0043-1354\(01\)00099-9](https://doi.org/10.1016/S0043-1354(01)00099-9))
25. Y. Liu, C. Sun, J. Xu, Y. Li, *J. Hazard. Mater.* **168** (2009) 156 (<https://doi.org/10.1016/j.jhazmat.2009.02.009>)
26. S. Dahiya, R. M. Tripathi, A. G. Hegde, *Bioresour. Technol.* **99** (2008) 179 (<https://doi.org/10.1016/j.biortech.2006.11.011>)
27. F. A. Ismail, A. Z. Aris, *Environ. Sci. Pollut. Res.* **21** (2014) 344 (<https://doi.org/10.1007/s11356-013-1906-4>)
28. C. Zhou, X. Gong, W. Zhang, J. Han, R. Guo, *Water Environ. Res.* **89** (2017) 817 (<https://doi.org/10.2175/106143017X14902968254854>)
29. Y. Gao, *Asian J. Chem.* **25** (2013) 8537 (<http://dx.doi.org/10.14233/ajchem.2013.14828A>).